Journal of Colloid and Interface Science 482 (2016) 89–94

Contents lists available at ScienceDirect

Journal of Colloid and Interface Science

journal homepage: www.elsevier.com/locate/jcis

Regular Article

Rapid electrostatics-assisted layer-by-layer assembly of near-infrared-active colloidal photonic crystals

Khalid Askar, Sin-Yen Leo, Can Xu, Danielle Liu, Peng Jiang *

Department of Chemical Engineering, University of Florida, Gainesville, FL 32611, United States

GRAPHICAL ABSTRACT

A rapid and scalable bottom-up technology has been developed for layer-by-layer assembling near-infrared-active colloidal photonic crystals consisting of micrometer-scale silica microspheres. This new electrostatics-assisted approach can enhance the crystal transfer speed of traditional Langmuir-Blodgett-based colloidal assembly technologies by nearly 2 orders of magnitude.

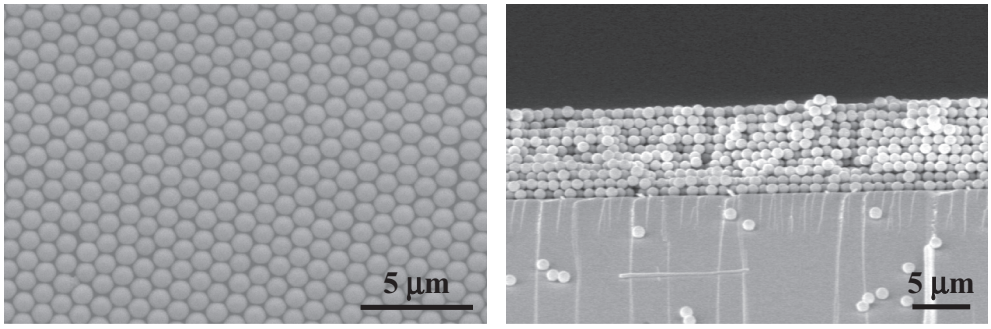

ARTICLE INFO

Article history:
Received 26 May 2016
Revised 16 July 2016
Accepted 28 July 2016
Available online 29 July 2016

Keywords:
Photonic crystals
Colloidal crystals
Self-assembly
Layer-by-layer
Langmuir-Blodgett
Electrostatics

ABSTRACT

Here we report a rapid and scalable bottom-up technique for layer-by-layer (LBL) assembling near-infrared-active colloidal photonic crystals consisting of large ($\geqslant 1$ μm) silica microspheres. By combining a new electrostatics-assisted colloidal transferring approach with spontaneous colloidal crystallization at an air/water interface, we have demonstrated that the crystal transfer speed of traditional Langmuir-Blodgett-based colloidal assembly technologies can be enhanced by nearly 2 orders of magnitude. Importantly, the crystalline quality of the resultant photonic crystals is not compromised by this rapid colloidal assembly approach. They exhibit thickness-dependent near-infrared stop bands and well-defined Fabry-Perot fringes in the specular transmission and reflection spectra, which match well with the theoretical calculations using a scalar-wave approximation model and Fabry-Perot analysis. This simple yet scalable bottom-up technology can significantly improve the throughput in assembling large-area, multilayer colloidal crystals, which are of great technological importance in a variety of optical and non-optical applications ranging from all-optical integrated circuits to tissue engineering.

1. Introduction

Photonic crystals are periodic dielectric materials that can control the flow of light in miniature volumes, promising for a wide

* Corresponding author.
E-mail address: pjiang@che.ufl.edu (P. Jiang).

http://dx.doi.org/10.1016/j.jcis.2016.07.076
0021-9797/

spectrum of optical applications, such as all-optical integrated circuits, lossless waveguides, and low-threshold lasers [1–3]. They also provide opportunities in exploring new physical phenomena like negative refractive index and suppression or enhancement of spontaneous emission [4,5]. Compared with complex and expensive top-down nanofabrication technologies (e.g., electron-beam lithography and focused ion-beam milling), bottom-up colloidal self-assembly renders a much simpler, faster, and cheaper approach for fabricating three-dimensionally (3-D) ordered photonic crystals operating at visible and near-infrared (NIR) wavelengths [6–11]. To enable full photonic band gaps, the replication of the self-assembled colloidal crystals in high refractive index materials (e.g., silicon) to create the so-called macroporous (or inverted) photonic crystals has been extensively exploited [12,13]. Because silica microspheres can survive the typical harsh templating conditions, such as high temperature in the chemical vapor deposition of silicon, a large variety of methodologies like convective self-assembly [14,15], gravitational sedimentation [16], spin-coating [17], electric or magnetic field-assisted assembly [9,18], and physical confinement [19,20] have been developed for assembling submicrometer-sized silica microspheres into 3-D colloidal crystals as sacrificial templates. However, spontaneous crystallization of large silica microspheres with diameter larger than 1 μm, which are needed for fabricating inverted photonic crystals operating at NIR telecommunication wavelengths, tends to be challenging, mainly due to the rapid gravitational sedimentation of large silica particles [12,21,22]. The same issue also hinders many other non-optical applications of self-assembled colloidal crystals consisting of μm-sized particles, such as in fabricating ordered macroporous membranes with large pores as 3-D scaffolds for tissue engineering and drug delivery [23].

Layer-by-layer transfer of monolayer colloidal crystals formed at an air/water interface, where the self-assembly process is induced by the high surface tension of water (72.75 mN/m at 20 °C), has been widely exploited as an effective methodology in fabricating multilayer colloidal photonic crystals with easily adjustable thicknesses [24–38]. Moreover, this Langmuir-Blodgett-based LBL technology enables the precise insertion of engineered artificial defects (e.g., planar defects) into 3-D photonic crystals, crucial for achieving active photonic crystal devices [39,40]. However, traditional LBL colloidal assembly approaches suffer from a few major drawbacks. They usually require sophisticated equipment (e.g., a Langmuir-Blodgett trough), and the process parameters (e.g., surface pressure and barrier speed) need to be precisely controlled to compress the floating microspheres into close-packed monolayers [30,41]. More importantly, a thin lubricating water layer between the transferred colloidal monolayer and the substrate greatly limits the substrate withdrawal speed. A typical upstroke speed of ~1 mm/min is widely used in previous studies to ensure conformal transfer of monolayer colloidal crystals onto various substrates [30,41,42]. A higher substrate withdrawal speed usually results in poor-quality colloidal crystals, or in the worst case scenario, no particle transfer onto the substrate. This slow crystal transfer speed significantly impedes the fabrication throughput of large-area colloidal photonic crystals, especially for assembling multilayer photonic crystals with many colloidal layers. For instance, it takes ~100 min to transfer a monolayer colloidal crystal to cover a 4-in.-sized substrate.

We have recently demonstrated a simple and scalable Langmuir-Blodgett-like bottom-up technology for assembling wafer-sized monolayer colloidal crystals onto both planar and non-planar substrates (e.g., multicrystalline silicon wafers) [43]. This approach does not require any sophisticated equipment and the process is easily controllable and highly reproducible. Unfortunately, similar to other Langmuir-Blodgett-based colloidal self-assembly techniques, the crystal transfer speed is very slow and it is limited to ~0.5 mm/min to deposit high-quality monolayer crystals. Here, we demonstrate that this speed can be greatly boosted to ~60 mm/min by simply using surface-modified substrates which possess opposite charges to the negatively charged silica microspheres. Multilayer colloidal photonic crystals consisting of large silica microspheres (diameter $\geqslant$ 1 μm) are then assembled in a LBL manner by this rapid approach. Critically, our optical characterization and modeling indicate that the crystalline quality of the resultant near-infrared-active photonic crystals is not compromised by the fast assembly process.

2. Experimental

2.1. Materials and substrates

Uniform silica microspheres with diameters of 1.0, 2.5, 3.5, and 8.0 μm made by a modified Stöber method are obtained from Particle Solutions LLC (Alachua, FL). These silica particles are cleaned by 6 cycles of repeated centrifugation followed by redispersion in 200-proof ethanol. The purified silica microspheres are used in preparing a colloidal suspension with 2 wt% of silica particles dispersed in ethylene glycol. A 75 × 25 mm glass microslide cleaned using a piranha solution (H_2SO_4:H_2O_2 = 4:1 by volume) at 70 °C for 60 min is rinsed with deionized water several times and then air-dried. The cleaned glass substrate is primed by 3-aminopropyltriethoxysilane (APS) using the well-established silane-coupling reactions [17,44], followed by rinsing with toluene and air drying. The amino groups of the surface-grafted APS molecules change the surface charges of the glass microslide from negative to positive. Deionized (DI) water (18.2 MΩ cm) is used directly from a Millipore A-10 water purification system.

2.2. Instrumentation

A KD Scientific 780-230 syringe pump is used to precisely control the withdrawal speed of the substrate in the Langmuir-Blodgett colloidal assembly process. Scanning electron microscopy (SEM) is carried out on a JEOL 6335F FEG-SEM. A thin layer of gold is sputtered onto the samples prior to imaging. Zeta potentials of silica microspheres are measured by a Brookhaven ZetaPlus unit. Fourier Transformed Infrared Spectroscopy (FTIR) is performed at normal incidence using a Thermo Electron Magna 760 spectrometer with a liquid-nitrogen-cooled mercury cadmium telluride detector.

2.3. Electrostatics-assisted LBL assembly of NIR-active colloidal photonic crystals

The functionalized glass substrate is then immersed in a glass Petri dish filled with deionized water. The colloidal silica-ethylene glycol suspension is added dropwise along the edge of the Petri dish. The suspension is spread immediately to form an iridescent colloidal crystal monolayer floating on the water surface [43]. Once the surface is completely covered with the floating silica microspheres, the functionalized glass microslide is vertically withdrawn at a rate of 60 mm/min controlled by the syringe pump, leading to the conformal transfer of the floating monolayer colloidal crystal onto both surfaces of the glass substrate. The strong electrostatic attraction between the positive APS-functionalized glass surfaces and the negatively charged silica microspheres (with a typical zeta potential of ~−40 mV) is critical in achieving this high coating speed. Our control experiments show that no particles are getting transferred onto negatively charged glass or silicon substrates with this high substrate withdrawal speed. Additionally, the electrostatic attraction makes the assembled particles adhere

strongly to the glass substrate, facilitating to enhance the mechanical stability of the self-assembled colloidal monolayers [45]. The coated glass slide is then placed into the same APS/toluene solution to functionalize the surfaces of the deposited silica microspheres, reverting the negative surface charges to positive. The surface-modified coating is then immersed into the same glass Petri dish and another colloidal layer is deposited. The same process can be repeated in a LBL manner to create 3-D ordered multilayer photonic crystals with well-defined numbers of colloidal layers. The layer numbers of the resultant crystals can be easily tuned by controlling the numbers of the surface functionalization/Langmuir-Blodgett assembly cycles.

3. Results and discussion

This novel electrostatics-assisted LBL self-assembly technology can greatly enhance the coating speed of the floating colloidal crystals, which is particularly important for improving the throughput in assembling large-area, multilayer photonic crystals. More importantly, the crystalline quality of the LBL-assembled photonic crystals is not compromised by the rapid colloidal transfer process.

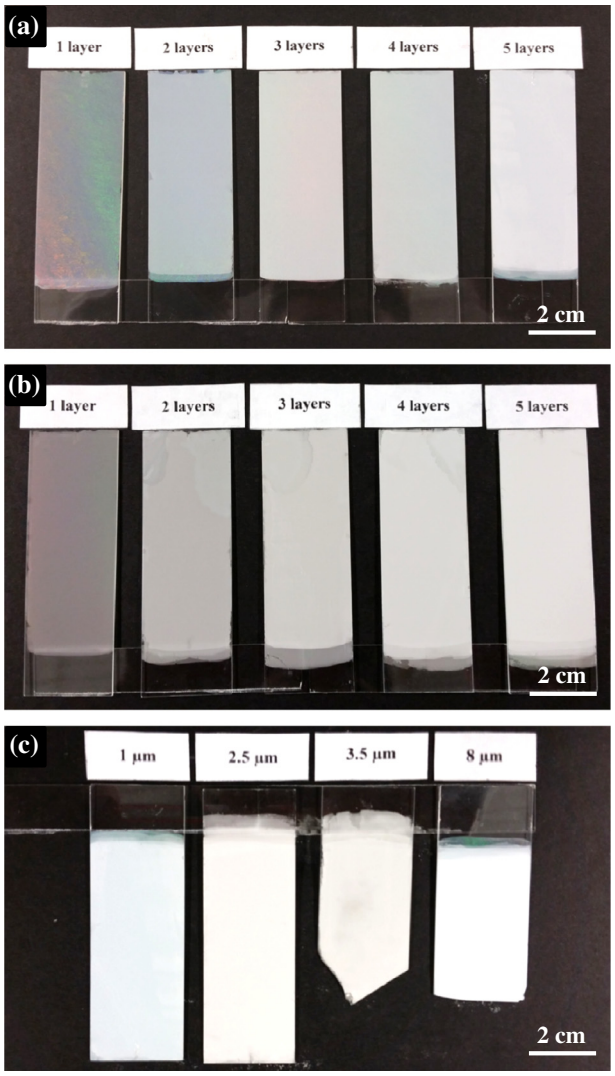

Fig. 1. Photographs of LBL-assembled colloidal photonic crystals. (a) 1.0 μm silica particles with different numbers of colloidal layers. (b) 2.5 μm silica particles with different numbers of colloidal layers. (c) 1.0, 2.5, 3.5, and 8.0 μm silica particles with 5 colloidal layers.

Fig. 1(a) shows a photograph of silica colloidal photonic crystals consisting of 1.0 μm microspheres with 1, 2, 3, 4, and 5 colloidal layers. All samples exhibit high coating uniformity over large areas. Moreover, the samples display angle-dependent iridescent colors caused by Bragg diffraction of visible light from the ordered colloidal arrays. Our extensive experiments further reveal that this simple LBL technology can be readily applied to assemble much larger silica microspheres. This is in sharp contrast to many existing colloidal self-assembly approaches which suffer from rapid gravitational sedimentation of large silica particles [12,21,22]. We have successfully assembled multilayer colloidal crystals using 2.5, 3.5, and 8.0 μm silica microspheres and their coating qualities are as good as the 1.0 μm ones (see Fig. 1(b) and (c)). We have also demonstrated that this electrostatics-assisted LBL technology can be easily scaled-up to make high-quality multilayer photonic crystals over wafer-sized areas. Fig. S1 in the supplementary material shows photographs of LBL-assembled photonic crystals consisting of 1 μm silica microspheres with 1, 2, 3, and 5 colloidal layers on 4-in.-sized silicon wafers. It only takes ~2 min to transfer a highly uniform colloidal monolayer to cover a 5-in.-sized glass or silicon substrate.

The high crystalline quality of the LBL-assembled photonic crystals is further confirmed by using scanning electron microscope (SEM). Fig. 2(a) shows a top-view SEM image of a transferred monolayer colloidal crystal consisting of 1.0 μm silica microspheres. The long-range hexagonal ordering of the crystal is evident from the image and the hexagonally arranged sharp peaks in the Fourier transform of a 100 μm^2 region (inset of Fig. 2(a)). Our extensive SEM imaging also reveals that the crystalline quality of the colloidal monolayers assembled using the rapid electrostatics-assisted LBL methodology is apparently higher than that of the colloidal crystals assembled using traditional Langmuir-Blodgett technology on bare glass or silicon substrates with native negative surface charges [43]. We speculate that the strong electrostatic attraction between the oppositely charged silica microspheres and the APS-modified substrates leads to the rapid immobilization of the transferred particles [45,46], which maintain the high crystalline quality of the monolayer colloidal crystal assembled at the air/water interface. By contrast, as shown in our previous work, the monolayer colloidal rafts transferred onto negatively charged substrates are still floating on a thin layer of water [43]. Capillary forces between neighboring microspheres induced by the evaporation of the residual water are thus dominating the final colloidal crystallization process. It is well-known that many types of defects, such as macroscopic cracks, can be introduced into the resultant crystals, mainly caused by the high internal stress induced by the evaporation of water [15,47].

Besides in-plane long-range order, the stacking of hexagonally close-packed colloidal layers perpendicular to the substrate is responsive for the diffraction observed in normal-incidence specular transmission and reflection measurements. Fig. 2(b) shows a top-view SEM image of an abraded region of a double-layer colloidal photonic crystal assembled by the electrostatics-assisted LBL technique. Although some intrinsic defects like point defects and grain boundaries are present, the top colloidal layer retains the hexagonal close-packed structure over the entire sample surface. Fig. 2(c)–(f) shows cross-sectional SEM images of LBL-assembled multilayer photonic crystals with 3, 4, 5, and 10 colloidal layers, respectively. These images reveal that the close-packed structure extends uniformly over all layers from top to bottom for all multilayer samples. In this close-packed geometry, whether the structure is face-centered cubic (ABCABC...), hexagonal close-packed (ABABAB...), or randomly stacked, these images illustrate that the LBL-assembled samples are oriented with their (1 1 1) crystalline planes parallel to the substrate. Importantly, our extensive SEM characterization shows that macroscopic cracks,

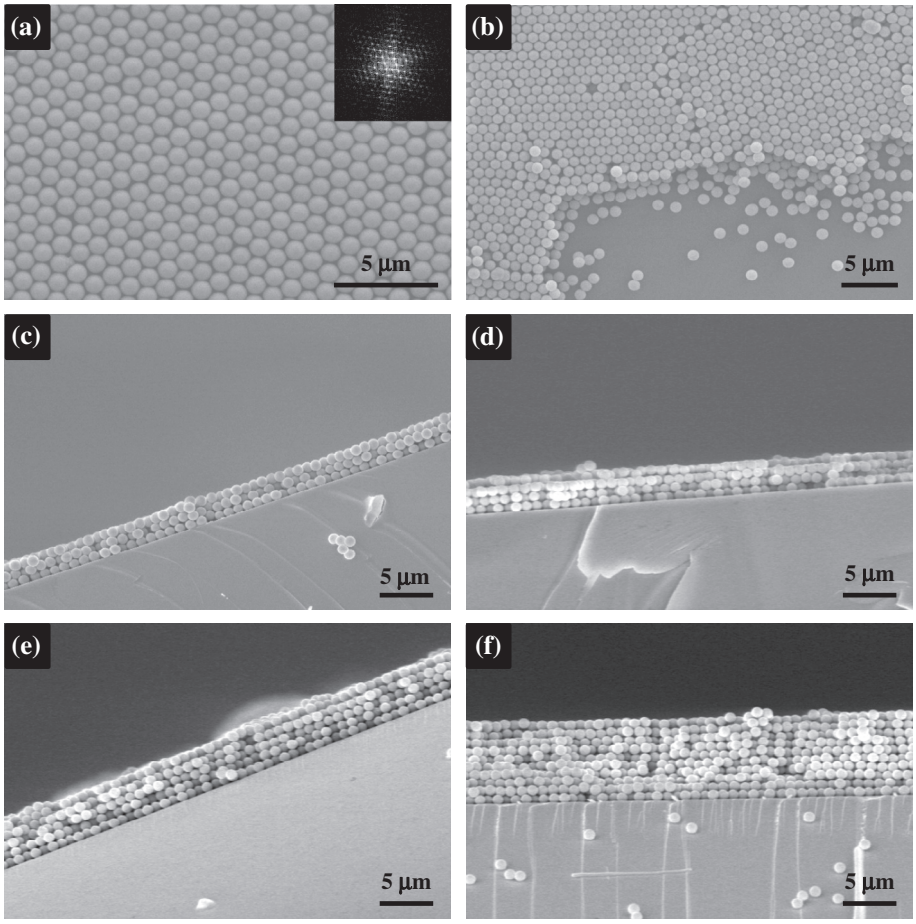

Fig. 2. SEM images of LBL-assembled colloidal photonic crystals consisting of 1.0 μm silica particles with different numbers of colloidal layers. (a) 1 layer. (b) 2 layers. (c) 3 layers. (d) 4 layers. (e) 5 layers. (f) 10 layers. The inset in (a) shows a Fourier transform of a 10 μm × 10 μm region.

which are commonly observed in colloidal crystals assembled by evaporation-induced processes (e.g., convective self-assembly) [15], can be completely excluded in all samples assembled by the new electrostatics-assisted LBL technique.

The specular transmission and reflection properties of the LBL-assisted colloidal photonic crystals are evaluated using the Thermo Electron Magna 760 Fourier Transform Infrared Spectroscopy. Fig. 3(a) and (b) shows the normal-incidence reflection and transmission spectra obtained from self-assembled colloidal photonic crystals consisting of 1.0 μm silica microspheres with 1, 2, 3, 4, 5, and 10 colloidal layers and a bare glass control sample. Distinct optical stop bands near 2300 nm, which are caused by the Bragg diffraction of NIR light from the 3-D ordered colloidal multilayers, are clearly shown in both transmission and reflection spectra. Additionally, the positions of the reflection peaks and the transmission dips match well with each other. Another notable feature of the spectra is the dependence of the bandwidth of the optical stop band with the number of colloidal layers of the LBL-assembled photonic crystals. The full-width-at-half-maximum (FWHM) of the reflection spectra in Fig. 3(a) is determined to be 938, 660, 538, 451, 410, and 277 nm for the crystals with 1, 2, 3, 4, 5, and 10 colloidal layers, respectively. The apparent narrowing of optical stop bands with increasing crystal thickness agrees with previous studies on self-assembled colloidal photonic crystals [48]. Moreover, we also use the optical characterization to evaluate the uniformity of the LBL-assembled colloidal photonic crystals by obtaining transmission and reflection spectra from multiple spots on the same sample. The spectra overlap well with each other, confirming the outstanding uniformity of the resultant photonic crystals over large areas.

To gain better understanding of the optical properties of the LBL-assembled NIR-active colloidal photonic crystals, optical simulations based on a scalar-wave approximation (SWA) model are performed to complement the experimental optical measurements. In the SWA theory, Maxwell's equations are solved for a periodic dielectric assuming that one may neglect diffraction from all but one set of crystalline planes (for example, the (1 1 1) planes in our current case) [48]. The SWA calculations contain no adjustable parameters as the size of the silica microspheres and the number of colloidal layers can be well controlled, and the refractive indices of the silica particles and air are known. Fig. 4(a) compares the experimental and SWA-simulated reflection spectra for 1.0 μm-diameter colloidal photonic crystals with 4, 5, and 10 colloidal layers. The experimental and theoretical spectra match extremely well in nearly all spectral aspects, such as peak position, amplitude, and bandwidth. The strong dependence of the bandwidth of the optical stop band on the crystal thickness (i.e., number of colloidal layers) is also evident from the simulations. As a perfect face-centered cubic crystal lattice is used in the SWA modeling, the excellent match between the experimental and theoretical spectra further confirms the high crystalline quality of the LBL-assembled colloidal photonic crystals.

In addition to distinct optical stop bands originated from the Bragg diffraction of NIR light from 3-D ordered colloidal multilayers, well-defined Fabry-Perot fringes are clearly shown in the optical spectra (see Fig. 3). These fringes result from interference

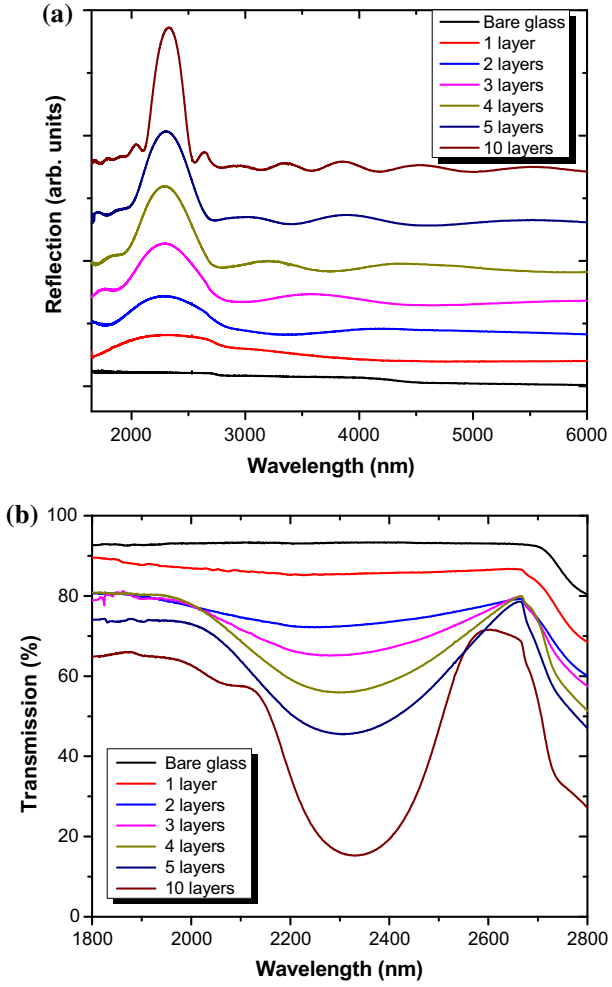

Fig. 3. Normal incidence (a) reflection and (b) transmission spectra obtained from LBL-assembled colloidal photonic crystals consisting of 1.0 μm silica particles with different numbers of colloidal layers. These spectra have been vertically offset for clarity.

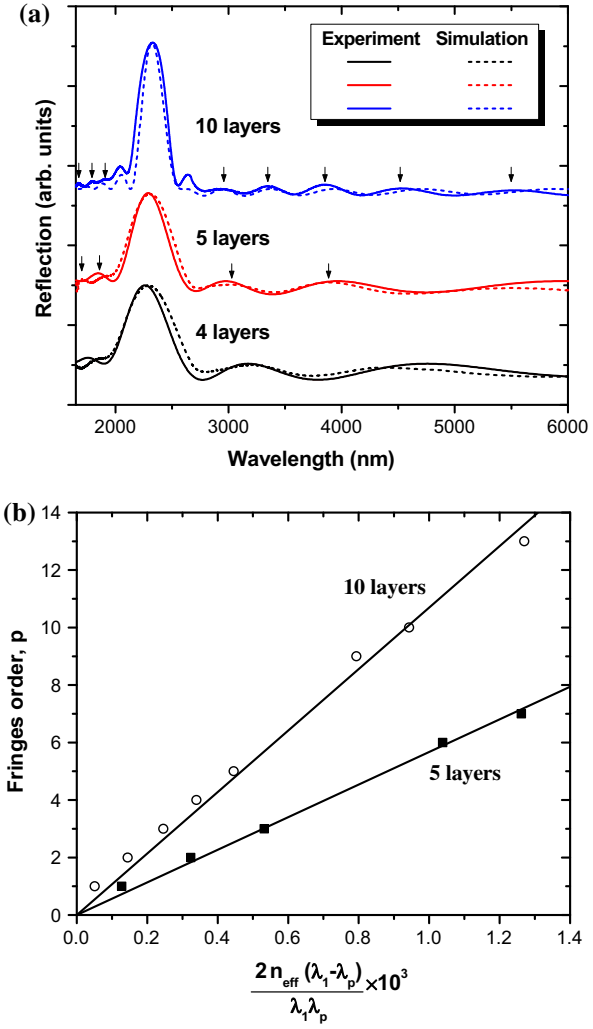

Fig. 4. (a) Comparison between the experimental (solid) and SWA-simulated (dotted) reflection spectra for colloidal photonic crystals consisting of 1.0 μm silica particles with 4, 5, and 10 colloidal layers. The arrows indicate local Fabry-Perot maxima, λ_p, chosen for thickness analysis. (b) Fringe order, p, versus Fabry-Perot maxima position, for LBL-assembled colloidal photonic crystal with 5 and 10 colloidal layers.

between reflections from the top and bottom surfaces of the photonic crystals and are indicated by the arrows in Fig. 4(a). The spectral positions of these local maxima can be predicted using Bragg's law. At normal incidence, one particular FP maximum (e.g., the one at the longest wavelength) occurs at a wavelength, λ_1, given by:

$$p_1\lambda_1 = 2n_{eff}T \quad (1)$$

Here, p_1 is an integer, n_{eff} is the effective refractive index of the colloidal photonic crystal and T is the crystal thickness. Subsequent maxima appear at shorter wavelengths:

$$(p + p_1)\lambda_p = 2n_{eff}T \quad (2)$$

p is a positive integer numbering consecutive maxima from the long-wavelength fringe, p_1. Rearranging Eqs. (1) and (2) gives the fringe order, p:

$$p = \frac{2n_{eff}(\lambda_1 - \lambda_p)}{\lambda_1\lambda_p}T \quad (3)$$

Thus, a plot of p versus $2n_{eff}(\lambda_1-\lambda_p)/\lambda_1\lambda_p$ gives a straight line with a slope of T. This linear relationship is clearly shown by the FP analysis for the 5-layer and 10-layer samples in Fig. 4(b). The good agreement between the experimental FP maxima and the theoretical predictions (straight lines) is a further testimony of the superior crystalline quality of the NIR-active photonic crystals assembled by the rapid LBL technique.

4. Conclusions

In conclusion, we have developed a new electrostatics-assisted LBL assembly technology for rapidly and scalably fabricating high-quality, NIR-active colloidal photonic crystals consisting of large silica microspheres, which are otherwise difficult to be assembled by traditional bottom-up techniques. The Langmuir-Blodgett-based crystal transfer speed can be enhanced by nearly two orders of magnitude by this electrostatics-assisted approach, while the crystalline quality of the resultant crystals is not compromised by the rapid assembly process. Our preliminary experiments have shown that this scalable technology can be applied to assemble silica nanoparticles as small as 100 nm diameter. In addition to precisely controlling the structural parameters of colloidal photonic crystals (e.g., thickness and engineered defects), this scalable methodology could find many important optical and non-optical

applications ranging from antireflection coatings to tissue engineering [23,49,50].

Acknowledgments

This work was partially supported by the US Defense Threat Reduction Agency, Basic Research Award # HDTRA1-15-1-0022, to University of Florida and an Early Stage Innovations grant (Award No. NNX14AB07G) from NASA's Space Technology Research Grants Program. Acknowledgments were also made to the US National Science Foundation (NSF) under Award No. CMMI-1300613.

Appendix A. Supplementary material

Supplementary data associated with this article can be found, in the online version, at http://dx.doi.org/10.1016/j.jcis.2016.07.076.

References

[1] J.D. Joannopoulos, P.R. Villeneuve, S.H. Fan, Photonic crystals: putting a new twist on light, Nature 386 (1997) 143–149.
[2] J.F. Galisteo-Lopez, M. Ibisate, R. Sapienza, L.S. Froufe-Perez, A. Blanco, C. Lopez, Self-assembled photonic structures, Adv. Mater. 23 (2011) 30–69.
[3] Y. Yin, J. Ge, Themed issue: the chemistry of photonic crystals and metamaterials, J. Mater. Chem. C 1 (2013) 6001–6002.
[4] N. Kaina, F. Lemoult, M. Fink, G. Lerosey, Negative refractive index and acoustic superlens from multiple scattering in single negative metamaterials, Nature 525 (2015) 77–81.
[5] M. Fujita, S. Takahashi, Y. Tanaka, T. Asano, S. Noda, Simultaneous inhibition and redistribution of spontaneous light emission in photonic crystals, Science 308 (2005) 1296–1298.
[6] E. Armstrong, C. O'Dwyer, Artificial opal photonic crystals and inverse opal structures - fundamentals and applications from optics to energy storage, J. Mater. Chem. C 3 (2015) 6109–6143.
[7] G. von Freymann, V. Kitaev, B.V. Lotschz, G.A. Ozin, Bottom-up assembly of photonic crystals, Chem. Soc. Rev. 42 (2013) 2528–2554.
[8] F. Li, D.P. Josephson, A. Stein, Colloidal assembly: the road from particles to colloidal molecules and crystals, Angew. Chem. Int. Ed. 50 (2011) 360–388.
[9] J. Ge, Y. Yin, Responsive photonic crystals, Angew. Chem. Int. Ed. 50 (2011) 1492–1522.
[10] O.D. Velev, S. Gupta, Materials fabricated by micro- and nanoparticle assembly - the challenging path from science to engineering, Adv. Mater. 21 (2009) 1897–1905.
[11] D. Yang, S. Ye, J. Ge, Solvent wrapped metastable colloidal crystals: highly mutable colloidal assemblies sensitive to weak external disturbance, J. Am. Chem. Soc. 135 (2013) 18370–18376.
[12] Y.A. Vlasov, X.Z. Bo, J.C. Sturm, D.J. Norris, On-chip natural assembly of silicon photonic bandgap crystals, Nature 414 (2001) 289–293.
[13] B.T. Holland, C.F. Blanford, A. Stein, Synthesis of macroporous minerals with highly ordered three-dimensional arrays of spheroidal voids, Science 281 (1998) 538–540.
[14] B.G. Prevo, O.D. Velev, Controlled, rapid deposition of structured coatings from micro- and nanoparticle suspensions, Langmuir 20 (2004) 2099–2107.
[15] P. Jiang, J.F. Bertone, K.S. Hwang, V.L. Colvin, Single-crystal colloidal multilayers of controlled thickness, Chem. Mater. 11 (1999) 2132–2140.
[16] R. Mayoral, J. Requena, J.S. Moya, C. Lopez, A. Cintas, H. Miguez, F. Meseguer, L. Vazquez, M. Holgado, A. Blanco, 3D long-range ordering in an SiO_2 submicrometer-sphere sintered superstructure, Adv. Mater. 9 (1997) 257–260.
[17] P. Jiang, M.J. McFarland, Large-scale fabrication of wafer-size colloidal crystals, macroporous polymers and nanocomposites by spin-coating, J. Am. Chem. Soc. 126 (2004) 13778–13786.
[18] J. Kleinert, S. Kim, O.D. Velev, Electric-field-assisted convective assembly of colloidal crystal coatings, Langmuir 26 (2010) 10380–10385.
[19] Z. Cai, J. Teng, D. Xia, X.S. Zhao, Self-assembly of crack-free silica colloidal crystals on patterned silicon substrates, J. Phys. Chem. C 115 (2011) 9970–9976.
[20] J. Zhang, A. Alsayed, K.H. Lin, S. Sanyal, F. Zhang, W.J. Pao, V.S.K. Balagurusamy, P.A. Heiney, A.G. Yodh, Template-directed convective assembly of three-dimensional face-centered-cubic colloidal crystals, Appl. Phys. Lett. 81 (2002) 3176–3178.
[21] N. Vogel, S. Utech, G.T. England, T. Shirman, K.R. Phillips, N. Koay, I.B. Burgess, M. Kolle, D.A. Weitz, J. Aizenberg, Color from hierarchy: diverse optical properties of micron-sized spherical colloidal assemblies, Proc. Natl. Acad. Sci. USA 112 (2015) 10845–10850.
[22] S. Wong, V. Kitaev, G.A. Ozin, Colloidal crystal films: advances in universality and perfection, J. Am. Chem. Soc. 125 (2003) 15589–15598.
[23] C.F.C. Joao, J.M. Vasconcelos, J.C. Silva, J.P. Borges, An overview of inverted colloidal crystal systems for tissue engineering, Tissue Eng. B 20 (2014) 437–454.
[24] L.N.D. Kallepalli, C. Constantinescu, P. Delaporte, O. Uteza, D. Grojo, Ultra-high ordered, centimeter scale preparation of microsphere Langmuir films, J. Colloid Interface Sci. 446 (2015) 237–243.
[25] M. Bardosova, P. Hodge, L. Pach, M.E. Pemble, V. Smatko, R.H. Tredgold, D. Whitehead, Synthetic opals made by the Langmuir-Blodgett method, Thin Solid Films 437 (2003) 276–279.
[26] D. Nagao, R. Kameyama, H. Matsumoto, Y. Kobayashi, M. Konno, Single- and multi-layered patterns of polystyrene and silica particles assembled with a simple dip-coating, Colloid Surf. A 317 (2008) 722–729.
[27] M. Bardosova, M.E. Pemble, I.M. Povey, R.H. Tredgold, The Langmuir-Blodgett approach to making colloidal photonic crystals from silica spheres, Adv. Mater. 22 (2010) 3104–3124.
[28] M. Bardosova, F.C. Dillon, M.E. Pemble, I.M. Povey, R.H. Tredgold, Langmuir-Blodgett assembly of colloidal photonic crystals using silica particles prepared without the use of surfactant molecules, J. Colloid Interface Sci. 333 (2009) 816–819.
[29] L. Zhang, Z. Xiong, L. Shan, L. Zheng, T. Wei, Q. Yan, Layer-by-layer approach to (2+1)D photonic crystal superlattice with enhanced crystalline integrity, Small 11 (2015) 4910–4921.
[30] S.G. Romanov, M. Bardosova, M. Pemble, C.M.S. Torres, (2+1)-dimensional photonic crystals from Langmuir-Blodgett colloidal multilayers, Appl. Phys. Lett. 89 (2006) 043105.
[31] S.G. Romanov, M. Bardosova, I.M. Povey, M.E. Pemble, C.M.S. Torres, Understanding of transmission in the range of high-order photonic bands in thin opal film, Appl. Phys. Lett. 92 (2008) 191106.
[32] K.E. Tettey, M.Q. Yee, D. Lee, Layer-by-layer assembly of charged particles in nonpolar media, Langmuir 26 (2010) 9974–9980.
[33] M.-H. Lin, H.-Y. Chen, S. Gwo, Layer-by-layer assembly of three-dimensional colloidal supercrystals with tunable plasmonic properties, J. Am. Chem. Soc. 132 (2010) 11259–11263.
[34] X. Wang, Y. Wang, Q.M. Chen, Rapid facial fabrication of silica colloidal crystal film at the air/water interface, J. Nanosci. Nanotechnol. 15 (2015) 9711–9716.
[35] Y. Kusaka, N. Ishida, H. Ushijima, Role of interfacial interactions in ordering of two-dimensional colloidal self-assemblies on polyelectrolyte multilayer surfaces, Soft Matter 9 (2013) 3155–3163.
[36] F. Xue, S.A. Asher, Z.H. Meng, F.Y. Wang, W. Lu, M. Xue, F.L. Qi, Two-dimensional colloidal crystal heterostructures, RSC Adv. 5 (2015) 18939–18944.
[37] A. Gil, F. Guitian, Formation of 2D colloidal crystals by the Langmuir-Blodgett technique monitored in situ by Brewster angle microscopy, J. Colloid Interface Sci. 307 (2007) 304–307.
[38] Y.L. Lee, Z.C. Du, W.X. Lin, Y.M. Yang, Monolayer behavior of silica particles at air/water interface: a comparison between chemical and physical modifications of surface, J. Colloid Interface Sci. 296 (2006) 233–241.
[39] Y.X. Zhao, K. Wostyn, G. de Schaetzen, K. Clays, L. Hellemans, A. Persoons, M. Szekeres, R.A. Schoonheydt, The fabrication of photonic band gap materials with a two-dimensional defect, Appl. Phys. Lett. 82 (2003) 3764–3766.
[40] Q. Yan, L.K. Teh, Q. Shao, C.C. Wong, Y.-M. Chiang, Layer transfer approach to opaline hetero photonic crystals, Langmuir 24 (2008) 1796–1800.
[41] S. Reculusa, P. Masse, S. Ravaine, Three-dimensional colloidal crystals with a well-defined architecture, J. Colloid Interface Sci. 279 (2004) 471–478.
[42] S. Reculusa, S. Ravaine, Synthesis of colloidal crystals of controllable thickness through the Langmuir-Blodgett technique, Chem. Mater. 15 (2003) 598–605.
[43] B.M. Phillips, P. Jiang, B. Jiang, Biomimetic broadband antireflection gratings on solar-grade multicrystalline silicon wafers, Appl. Phys. Lett. 99 (2011) 191103.
[44] S.P. Pack, N.K. Kamisetty, M. Nonogawa, K.C. Devarayapalli, K. Ohtani, K. Yamada, Y. Yoshida, T. Kodaki, K. Makino, Direct immobilization of DNA oligomers onto the amine-functionalized glass surface for DNA microarray fabrication through the activation-free reaction of oxanine, Nucleic Acids Res. 35 (2007).
[45] J. Aizenberg, P.V. Braun, P. Wiltzius, Patterned colloidal deposition controlled by electrostatic and capillary forces, Phys. Rev. Lett. 84 (2000) 2997–3000.
[46] D. Lee, D. Omolade, R.E. Cohen, M.F. Rubner, pH-dependent structure and properties of TiO_2/SiO_2 nanoparticle multilayer thin films, Chem. Mater. 19 (2007) 1427–1433.
[47] Y. Huang, J. Zhou, B. Su, L. Shi, J. Wang, S. Chen, L. Wang, J. Zi, Y. Song, L. Jiang, Colloidal photonic crystals with narrow stopbands assembled from low-adhesive superhydrophobic substrates, J. Am. Chem. Soc. 134 (2012) 17053–17058.
[48] J.F. Bertone, P. Jiang, K.S. Hwang, D.M. Mittleman, V.L. Colvin, Thickness dependence of the optical properties of ordered silica-air and air-polymer photonic crystals, Phys. Rev. Lett. 83 (1999) 300–303.
[49] K.H. Nielsen, D.K. Orzol, S. Koynov, S. Carney, E. Hultstein, L. Wondraczek, Large area, low cost anti-reflective coating for solar glasses, Sol. Energy Mater. Sol. Cells 128 (2014) 283–288.
[50] J.A. Webb, R. Bardhan, Emerging advances in nanomedicine with engineered gold nanostructures, Nanoscale 6 (2014) 2502–2530.